Understanding Reactivity with Kohn–Sham Molecular Orbital Theory: E2–S_N2 Mechanistic Spectrum and Other Concepts

F. MATTHIAS BICKELHAUPT

Fachbereich Chemie, Philipps-Universität Marburg, Hans-Meerwein-Strasse, D-35032 Marburg, Germany

Received 10 August 1998; accepted 17 August 1998

ABSTRACT: On the basis of Kohn–Sham density functional (DFT) investigations on elementary organic and organometallic reactions, we show how a detailed understanding of the electronic structure of a reaction system can help recognize certain characteristics of the process, yielding valuable mechanistic concepts. The concept of the base as a selective catalyst in E2 eliminations, for example, leads to a straightforward explanation for the general preference for *anti* over *syn* stereochemistry in base-induced elimination reactions. Furthermore, electronic structure considerations provide the so-called E2–S_N2 mechanistic spectrum, in terms of which one can interpret and understand the competition between elimination and substitution reactions and the shift, on solvation, of the reactivity from E2 to S_N2. In addition, mechanistic concepts from organometallic and organic chemistry are linked as we argue that oxidative addition may be conceived, in some respect, as the organometallic analog of the frontside S_N2 substitution. Finally, we introduce the ideas of ''activation strain'' of and ''transition state interaction'' between the deformed reactants in the activated complex, which together determine the activation energy, $\Delta E^* = \Delta E^*_{\text{strain}} + \Delta E^*_{\text{int}}$. They prove to be helpful conceptual tools for understanding in detail how activation barriers and relative efficiencies of competing reaction mechanisms arise and how they may be affected (e.g., by changing reactants or by solvation). © 1999 John Wiley & Sons, Inc. J Comput Chem 20: 114–128, 1999

Keywords: elimination; density functional theory; mechanistic concepts; orbital interactions; oxidative addition; reaction mechanisms; reactivity; substitution

Correspondence to: e-mail: bickel@chemie.uni-marburg.de
Contract/grant sponsor: Deutsche Forschungsgemeinschaft

CCC 0192-8651 / 99 / 010114-15

Introduction

In the recent past, Kohn–Sham density functional theory (DFT) has evolved into what is now one of the major approaches in quantum chemistry.[1–4] It has become an indispensable tool for the prediction of various chemical properties, in particular structure and reactivity, of systems in molecular as well as solid-state chemistry. What is it that makes Kohn–Sham DFT so attractive? One important reason is definitely that it represents a first-principles method that combines a high efficiency (a favorable order N^3 or better scaling of the computational cost) with a relatively high, that is, chemical, accuracy (in the order of a few kilocalories per mole). However, in our opinion it is just as important that Kohn–Sham DFT constitutes a physically meaningful molecular orbital (MO) model.[4] This allows one not only to predict correctly the behavior and properties of realistic model systems but also to understand the predicted phenomena in terms of elementary physical concepts from MO theory,[5,6] such as electron-pair bonding, donor/acceptor interaction, and Pauli repulsion (and electrostatics are also contained in the model). Although, this will not be the subject of the present discourse, it is appropriate at this point to mention yet another quantum-chemical approach to bonding and reactivity that combines the quantitative element with a physical model of the chemical bond, namely, valence bond (VB) theory. An excellent overview of the possibilities of the VB model can be found in the work of Shaik.[7]

Recently, we have pointed out how Kohn–Sham MO theory yields a consistent description, precise and yet transparent, of chemical bonding and molecular structure.[4,8] In the present study, these considerations are extended to elementary chemical reactions in organic and organometallic chemistry. To this end, after a concise description of the approach (second section), the results of various recent investigations[9] on E2 eliminations (third section), S_N2 substitutions (fourth section), and oxidative addition reactions (i.e., the insertion of a metal center into a C—X bond; fifth section) are reexamined and discussed in the broader context of this review. The purpose is to show how a detailed understanding of the electronic structure of a reaction system, as well as the changes in bonding that occur as the reaction proceeds, can help recognize certain characteristics of the process under consideration, yielding valuable mechanistic concepts. Finally, we evaluate our findings and discuss future prospects (last section).

Kohn–Sham MO Model and Chemical Bonding

The purpose of this section is a brief overview of the essential features of the Kohn–Sham MO theory and how the chemical bond can be analyzed in this approach. More detailed discussions can be found elsewhere.[1,2,4,10] The basic postulate in Kohn–Sham DFT is that, for any system of N interacting electrons moving in an external potential, $\nu(\mathbf{r})$ (the electrostatic potential of the nuclei), there exists a local potential, $\nu_s(\mathbf{r})$, such that the density, $\rho_s(\mathbf{r}) = \Sigma_i|\phi_i|^2$, of a system of N noninteracting electrons is equal to the exact density, $\rho(\mathbf{r})$, of the interacting electron system. The Kohn–Sham orbitals (i.e., the one-electron wave functions of the noninteracting electrons) follow from the Kohn–Sham equations [eq. (1)]:

$$\left[-\tfrac{1}{2}\nabla^2 + \nu_s(\mathbf{r})\right]\phi_i = \varepsilon_i\phi_i \qquad (1)$$

Here, the Kohn–Sham potential, $\nu_s(\mathbf{r})$, describes all effects stemming from the electron–nuclear and electron–electron interactions. Not only does it contain the attractive potential, $\nu(\mathbf{r})$, of the nuclei and the classical Coulomb repulsion, $V_{Coul}(\mathbf{r})$, within the electron density, $\rho(\mathbf{r})$, but it also accounts for all exchange and correlation effects, which have been ''folded into'' the local exchange-correlation potential, $\nu_{xc}(\mathbf{r})$; that is, $\nu_s(\mathbf{r}) = \nu(\mathbf{r}) + V_{Coul}(\mathbf{r}) + \nu_{xc}(\mathbf{r})$. This leaves us with an effective one-electron formulation of the quantum many-body problem, which is used in essence by all current implementations of DFT. For some time, physical meaning of the Kohn–Sham orbitals has been denied. They were merely conceived as an instrument to conveniently construct the exact density, which could then be substituted into (a good approximation to) the Hohenberg–Kohn density functional to provide, in turn, the exact (or accurate) total energy: $E = E[\rho(\mathbf{r})]$. However, Baerends et al.[10] pointed out that Kohn–Sham orbitals do have a physical interpretation, that they are perfectly suited for the use in orbital theories of chemistry, and that they even have certain advantages over Hartree–Fock orbitals (see also ref. 4).

In the framework of Kohn–Sham MO theory, one can decompose an accurate bond energy be-

tween mono- and/or polyatomic fragments of a molecular system (say, a base and a substrate for E2 elimination; see third and fourth sections) into the contributions associated with the various orbital and electrostatic interactions. We follow here the extended transition-state (ETS) method developed by Ziegler and Rauk[11] (for related analyses in various MO approaches see ref. 12). First, the overall bond energy, ΔE, is divided into two major components [eq. (2)]: (i) the preparation energy, ΔE_{prep}, corresponding to the amount of energy required to deform the separated fragments, A and B say, from their equilibrium structure to the geometry they acquire in the overall molecule ($\Delta E_{prep,geo}$) and to excite them to the their valence electronic configuration ($\Delta E_{prep,el}$); and (ii) the actual interaction energy, ΔE_{int}, between the prepared fragments:

$$\begin{aligned}\Delta E &= \Delta E_{prep} + \Delta E_{int} \\ &= \Delta E_{prep,geo} + \Delta E_{prep,el} + \Delta E_{int} \end{aligned} \quad (2)$$

In the following step of the ETS analysis, the interaction energy, ΔE_{int}, is further decomposed into three physically meaningful terms [eq. (3)][4,11]:

$$\begin{aligned}\Delta E_{int} &= \Delta V_{elst} + \Delta E_{Pauli} + \sum_{\Gamma} \Delta E_{oi,\Gamma} \\ &= \Delta E^0 + \Delta E_{oi} \end{aligned} \quad (3)$$

The term ΔV_{elst} corresponds to the classical electrostatic interaction between the unperturbed charge distributions of the prepared fragments as they are brought together at their final positions, giving rise to an overall density that is simply a superposition of fragment densities $\rho_A + \rho_B$. For neutral fragments, ΔV_{elst} is usually attractive.[4] The Pauli repulsion ΔE_{Pauli} then arises as the energy change associated with going from $\rho_A + \rho_B$ to the wave function $\Psi^0 = NA[\Psi_A\Psi_B]$, which properly obeys the Pauli principle through explicit antisymmetrization (A operator) and renormalization (N constant) of the product of fragment wave functions. It comprises the four-electron destabilizing interactions between occupied orbitals and is responsible for any steric repulsion. In the case of neutral fragments, it may be useful to combine ΔV_{elst} and ΔE_{Pauli} in the steric interaction, ΔE^0 [eq. (3)]. Finally, the wave function is allowed to relax from Ψ^0 to the fully converged wavefunction Ψ. The associated orbital interactions ΔE_{oi} account for electron-pair bonding, charge transfer (e.g., HOMO–LUMO interactions), and polarization (empty/occupied orbital mixing on one fragment due to the presence of another fragment). They can be further decomposed into the contributions from each irreducible representation, Γ, of the interacting system [eq. (3)]. In systems with a clear σ/π separation, this symmetry partitioning proves to be most informative.

Elimination Reactions: Base as Selective Catalyst

Base-induced 1,2-elimination (E2) [eq. (4a)] and nucleophilic substitution (S_N2) [eq. (4b)] constitute two fundamental types of chemical reactions and are of considerable importance in organic synthesis.[13] They have been thoroughly investigated in condensed[14] and gas-phase[15–18] experiments as well as in theoretical studies.[19,20] Principally, E2 elimination is always in competition with S_N2 substitution and the two pathways may occur as unwanted side reactions of each other. Therefore, a true understanding of the factors that determine the course of these processes is important for the design of efficient syntheses:

$$B^- + H\text{—}\overset{\beta}{C}R_2\text{—}\overset{\alpha}{C}R_2\text{—}L \xrightarrow{E2} B\text{—}H + CR_2{=}CR_2 + L^- \quad (4a)$$

$$B^- + H\text{—}\overset{\beta}{C}R_2\text{—}\overset{\alpha}{C}R_2\text{—}L \xrightarrow{S_N2} H\text{—}CR_2\text{—}CR_2\text{—}B + L^- \quad (4b)$$

The nature of E2 reactions is now well understood and interpreted in terms of a variable transition state (VTS).[13,14] According to this concept, reactions are categorized according to the geometry of the transition state (TS), which is conceived as being located at one point in a continuous spectrum of mechanistic possibilities. The VTS theory for E2 reactions comprises the Bunnett–Cram E2H spectrum[14d,e] involving linear proton transfer (Scheme 1) and the Winstein–Parker E2H–E2C spectrum[14f–h] in which bent proton transfer may occur with a certain degree of covalent base/C^α interaction (Scheme 2).

In this section, we focus on the stereochemistry of E2 eliminations. Why do they proceed preferentially via a coplanar H^β—C^β—C^α—L arrangement of the substrate, and why does *anti* elimination generally prevail over *syn* elimination (Scheme 3)? Let us consider the *anti*-E2 and *syn*-E2 pathways of the simple model reaction between a fluo-

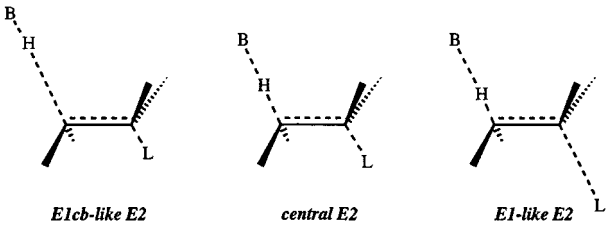

SCHEME 1. The Bunnett–Cram E2H mechanistic spectrum.

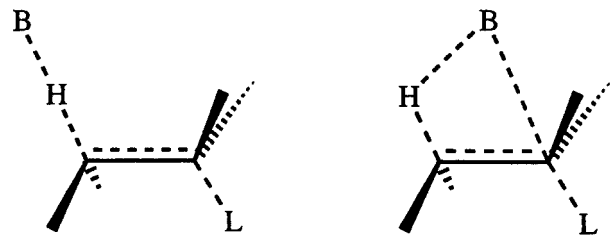

SCHEME 2. The Winstein–Parker E2H–E2C mechanistic spectrum.

ride anion as base and fluoroethane as substrate, $F^- + C_2H_5F$, which has been investigated at the BVWN-Stoll/TZ2P//Xα/DZP level of theory[9a] (we note that the conclusions of ref. 9a are confirmed by the preliminary results of a recent BP86/TZ2P study[9c]). In Scheme 3, the schematic reaction energy profiles for these processes are shown.

The first step in the reaction is the exothermic formation of a reactant complex. In the most stable one, $[F^-, C_2H_5F]$, the base binds by -10.6 kcal/mol to the C^{β}—H bond that is trans to the C^{α}—F bond (see Fig. 1). This complex is predestined to react further via *anti* elimination. In the complex for *syn* elimination, which is a few kilocalories per mole less stable, the base is connected to a C^{β}—H bond that is oriented *gauche* to the C^{α}—F bond (not shown in figure). The occurrence of stable reactant complexes is a typical feature of gas-phase ion/molecule reactions. This phenomenon becomes less important on solvation and may disappear completely in the condensed phase (see fourth section). From the respective reactant complexes, the reaction proceeds either via the *anti*-E2 or the *syn*-E2 transition state, yielding, in both cases, $C_2H_4 + FHF^-$, in which the leaving group and conjugate acid form a stable complex, as the most stable products with an overall reaction energy of -40.4 kcal/mol (for comparison, the formation of $HF + C_2H_4 + F^-$ is endothermic by 6.7 kcal/mol). The activation energy for the *anti*-E2 elimination (-9.5 kcal/mol) is clearly lower than that for the *syn*-E2 pathway (-0.5 kcal/mol, Table I). Note that whereas the TSs are higher in energy than the corresponding reactant complexes, they are below the reactants, as reflected by the negative activation energies.[18] This is another peculiarity that often goes with gas-

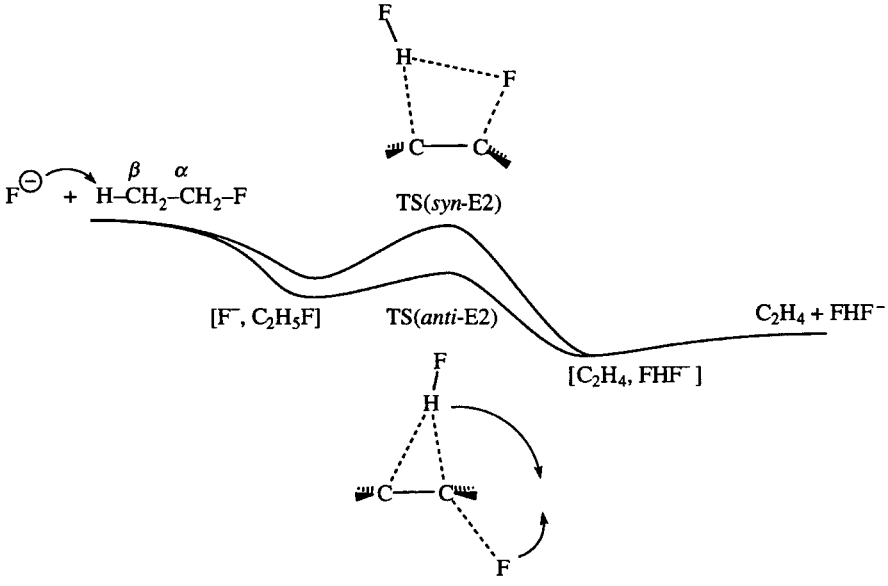

SCHEME 3. Reaction energy profiles for *anti*- and *syn*-E2 elimination.

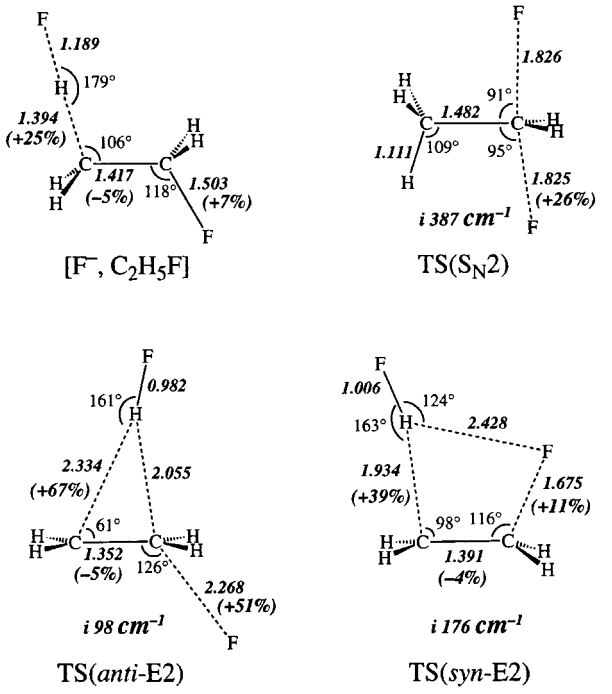

FIGURE 1. Geometries (in angstroms and degrees) for selected species on the E2 and S_N2 potential energy surface of $F^- + C_2H_5F$, together with imaginary frequencies for transition states ($X\alpha$/DZP level). Bond elongations (in percent) are given for [F^-, C_2H_5F] with respect to C_2H_5F and for the transition states with respect to [F^-, C_2H_5F].

phase ion/molecule reactions. In general, the barriers again become positive on solvation (see fourth section).

Why is the *syn*-E2 transition state higher in energy than that for *anti*-E2 elimination? A plausible reason might be the increased repulsion associated with the eclipsed conformation of the substrate, but this argument turns out to be erroneous. First, eclipsed fluoroethane is only 2.3 kcal/mol higher in energy than the staggered conformer; this does not account for the difference of 9 kcal/mol in activation energies. But, more importantly, it is the difference in energy between the deformed substrates in the respective *transition states* that counts in this context, and *not* the relative energy of the staggered and eclipsed conformers of the isolated fluoroethane reactant. The *syn* elimination reaches the TS at a point where the C_2H_5F substrate is much less deformed than in the *anti*-E2 transition state. This is simply due to the fact that in TS (*syn*-E2) the conjugate acid and the leaving group are located directly in front of each other. After a slight internal rotation and only a ''moderate'' elongation of the C^β—H and C^α—F bonds (by 39% and 11%, respectively; see Fig. 1) the abstracted proton and the leaving group can start to interact and stabilize the system and the energy does not rise further; that is, the transition state is reached. Such a stabilizing interaction is not possible in an early stage of the *anti* elimination, and TS (*anti*-E2) is reached somewhat later, after a much stronger elongation of the C^β—H and C^α—F bonds (by 67% and 51%, respectively). Note also the shift of the abstracted β-proton from C^β to C^α as the conjugate acid begins to migrate toward the leaving group in order to form the stable FHF^- complex. In fact, during some stage of the process, this movement occurs nearly unhindered on a very flat region or plateau of the potential energy surface.[9b,c] Thus, if we just compare the ''activation strain'' in the substrate (i.e., the deformation energy associated with bringing C_2H_5F into the geometry of the TS), it is the *syn* elimination with 83 kcal/mol that should be the more favorable process and *not* the *anti* elimination with 126 kcal/mol (Table I). We note that this ''activation strain'' or deformation energy of the substrate may be conceived as a good estimate of the barrier for the corresponding thermal elimination (i.e., without the assistance of a base) of HF from fluoroethane, which indeed occurs in a *syn* fashion (Scheme 4).[21] So, it is the interaction with the base that leads to the preference for *anti* elimination. This may be conceived as a textbook example of a catalytic process where the base is a selective catalyst that favors the high-energy process (see Scheme 4; UTS refers to the thermal or ''uncatalyzed'' TS). However, one restriction applies to this analogy: the base is not recovered after elimination has taken place. The catalyst is, in a sense, poisoned with a product molecule (HF) and is therefore needed in stoichiometric amounts.

But still the question remains *why* the base preferentially stabilizes the highly energetic transition structure for *anti* elimination, UTS (*anti*-E). This becomes clear as we take a closer look at the

TABLE I.
Activation Energies for F^- Base-Induced and ''Thermal'' Elimination of HF from C_2H_5F.[a]

Reaction	*Anti* elimination	*Syn* elimination
Base-induced	−9.5	−0.5
Without base[b]	126.4	83.0

[a] In kilocalories per mole; BVWN-Stoll/TZ2P//$X\alpha$/DZP.
[b] Refers to substrate C_2H_5F deformed to its geometry in the corresponding E2 transition state.

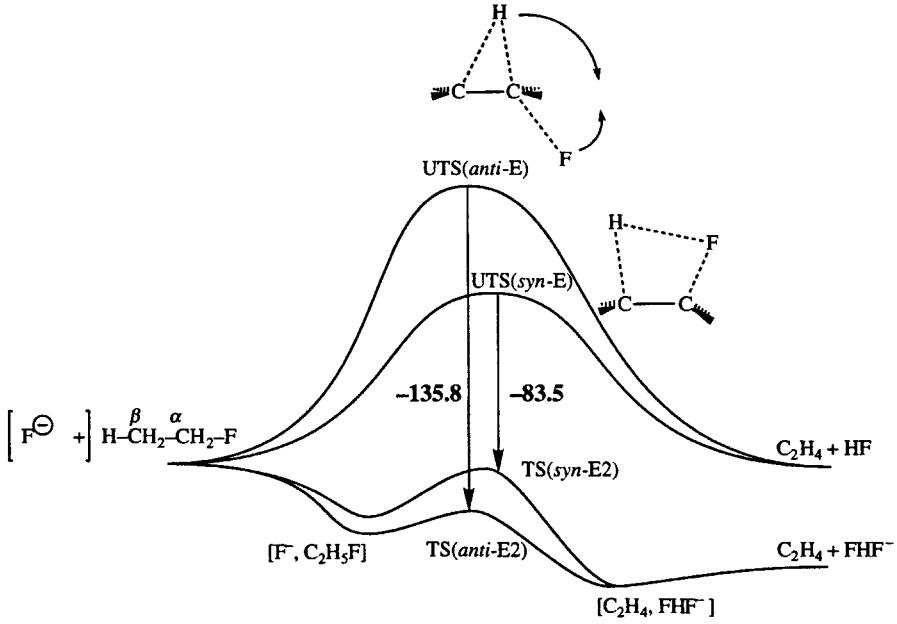

SCHEME 4. Catalytic effect (in kilocalories per mole) of the base on *anti*- and *syn*-E2 elimination.

substrate's LUMO, which is the acceptor orbital in the interaction with the HOMO of the base. It is basically the π-bonding combination between the lowest unoccupied e_x^* orbitals[6a,b,8d] of the $CH_3\cdot$ and the $\cdot CH_2F$ fragments, which have C—H and C—F antibonding character. This somewhat simplified picture is shown in Scheme 5 (for clarity, we use C_{3v} symmetry labels for the two C_s-distorted methyl fragments).

Thus, as the C^{β}—H and C^{α}—F bonds are elongated, the antibonding character of the LUMO is reduced and it decreases in energy (see Fig. 2). This is the key to the answer of our question. The LUMO of the strongly deformed substrate *anti*-TS is much lower in energy (by some 2.2 eV) than that in the *syn*-TS and, therefore, enters a significantly

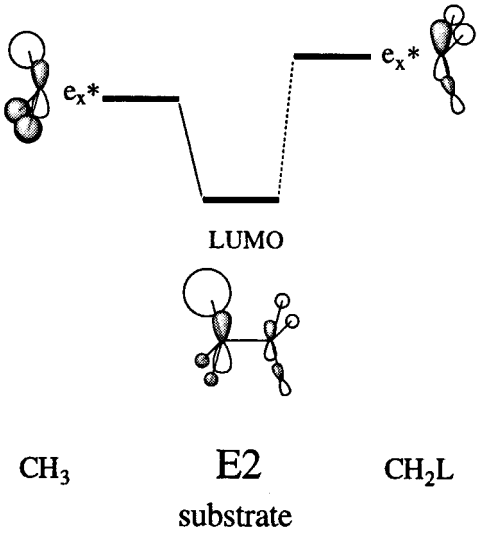

SCHEME 5. A substrate LUMO predestined for protophilic attack at H^{β}.

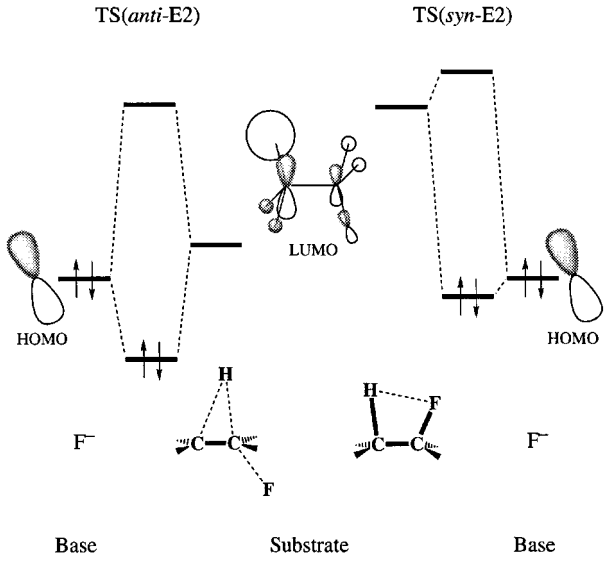

FIGURE 2. HOMO–LUMO interactions between the base (F^-) and the deformed substrate (C_2H_5F) in the *anti*-E2 and *syn*-E2 transition states. The lower energy LUMO of the strongly deformed substrate in the *anti*-E2 transition state leads to a more stabilizing interaction with the HOMO of the base.

more stabilizing donor–acceptor interaction with the HOMO of the base.[22] Note that the higher degree of substrate deformation inherently connected with the *anti* elimination is responsible for both, the high ''activation strain'' of the substrate and (due to the low energy of the substrate's LUMO) the even stronger interaction with the base.

The tendency to adopt a coplanar arrangement of the C^{β}—H and C^{α}—F bond, either *anti* or *syn*, can be understood on the basis of the C—C π-bonding character of the substrate LUMO. In that case, the π overlap is optimal, leading to a low LUMO energy and thus a strong interaction with the base HOMO.

Substitution Reactions: E2–S_N2 Mechanistic Spectrum

So far, we have concentrated on the stereochemistry of E2 eliminations. In this section, we examine the competition of base-induced *anti* elimination with nucleophilic S_N2 substitution [eq. (4)] and the influence of (micro)solvation.[9a,b] Scheme 6 shows the respective reaction energy profiles for our model system $F^- + C_2H_5F$.

Starting from the same reactant complex [F^-, C_2H_5F] from which E2 elimination may proceed, the base can also move toward the backside of the α-methyl group and perform a nucleophilic attack at C^{α}. This brings us to the transition state for S_N2 substitution (Fig. 1). The activation energy for S_N2 substitution (−0.5 kcal/mol) is again higher than that for E2 elimination (−9.5 kcal/mol, see Table II), in line with the experimental observation that (anionic) eliminations strongly dominate substitution in the gas phase.[15–17a,b] Overall, the substitution reaction is symmetric (products and reactants are equal) and therefore thermoneutral.

Before we try to explain the preference of E2 over S_N2 reaction in the gas phase, we note that, in the condensed phase, this relative order is reversed, or shifted in favor of substitution.[13,14] Furthermore, the absolute rate of both processes decreases drastically, by up to 20 orders of magnitude.[17b] We have tried to model these solvent effects theoretically by microsolvation[23–25] (i.e., by the introduction of only a few, one or two, HF molecules as models for protic solvent molecules). Many solvation modes are conceivable.[9b] Here, we examine the effect of mono- and disolvation of the F^- base. Already the introduction of one single HF solvent molecule causes a number of striking changes in the reaction energy profile and the trend further continues as the second solvent molecule is brought into play (see Table II and Fig. 3). Let us first mention two general microsolvation effects: (i) the wells of the reactant and product complexes become very shallow (e.g., the disolvated [F^-, C_2H_5F] is bound by only 0.7 kcal/mol); and (ii) the activation energies that were negative are now becoming positive. This is due to the differential solvation of reactants (which are strongly stabilized) and transition states (which

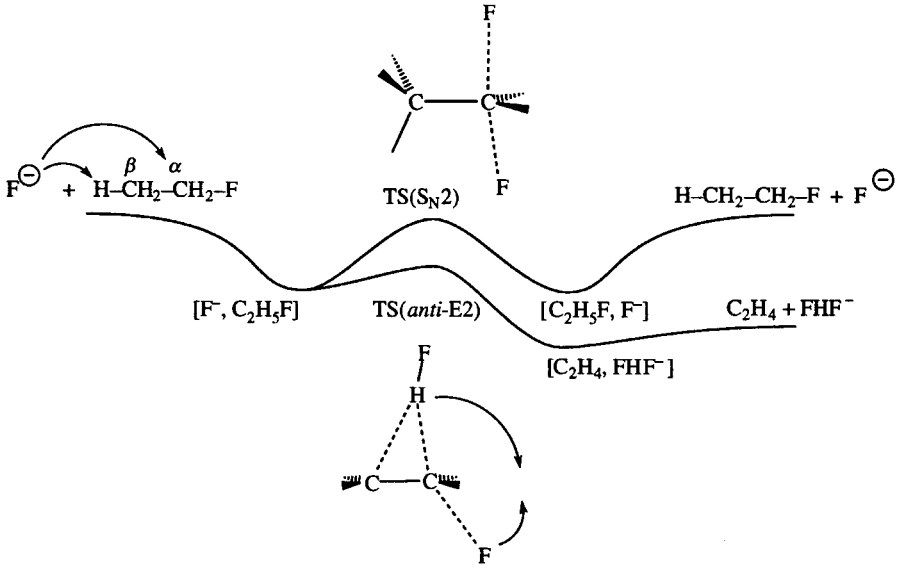

SCHEME 6. Reaction energy profiles for S_N2 substitution and *anti*-E2 elimination.

TABLE II.
Activation Energies for E2 and S_N2 Reactions of $F^- + C_2H_5F$.[a]

Reaction	E2[b]	S_N2
Gas phase	−9.5	−0.5
Monosolvated base	31.6	23.0
Disolvated base	54.4	34.4

[a] In kilocalories per mole; BVWN-Stoll/TZ2P//Xα/DZP.
[b] *Anti* elimination.

are weakly stabilized, see Fig. 3). In the former, the charge is localized on the base, which also has a high energy HOMO, leading to relatively strong electrostatic and charge-transfer interactions with solvent molecules. This stabilization is weakened in the intermediate complexes and, especially, in the transition states as the charge is more delocalized over the entire reaction system and the HOMO of the base is stabilized through its interaction with the substrate LUMO. Thus, only one or two solvent molecules bring us from the double-well potential, typical for the gas phase, to a nearly unimodal reaction energy profile that is characteristic for reactions in the condensed phase. Of course, we are still far removed from a real condensed-phase reaction which takes place in bulk solvent. But this result shows that some very important effects occur in the first solvation shell. Interestingly, we also find the reversal of activation energies (Fig. 3): on disolvation, for example, the S_N2 barrier is 20 kcal/mol lower than the E2 barrier (Table II).

Now, we return to the question of *why* the intrinsic reactivity of $F^- + C_2H_5F$ favors elimination. Similar to the approach followed earlier for *anti* and *syn* eliminations, we begin by inspecting the activation strain of the substrate in the *anti*-E2 and S_N2 transition states. As pointed out before, the *anti*-E2 transition state is strongly deformed, and much energy (126 kcal/mol, Table I) is needed to distort the substrate to the associated geometry. The S_N2 transition state, on the other hand, is much less deformed and tighter: a new C^α—F bond is already being formed to quite an extent (d_{CF} = 1.826 Å), whereas the old one is elongated only moderately (by 26%, Fig. 1). Accordingly, as shown in Figure 4, the activation strain of the substrate in TS(S_N2) is rather low, only some 31 kcal/mol (not given in table). Yet, the process is energetically unfavorable because of the significantly weaker and less stabilizing donor–acceptor interaction between the LUMO of the slightly deformed substrate (which is at high energy) and the HOMO of the F^- nucleophile (see Fig. 5, solid lines).

On solvation, however, the F^- HOMO is stabilized, resulting in a decrease of the interaction with the substrate LUMO (Fig. 5, dashed lines). Whereas this HOMO–LUMO interaction as such remains the strongest for the E2 transition state, the *weakening* in this stabilizing interaction on solvation of the base is, in absolute terms, the largest

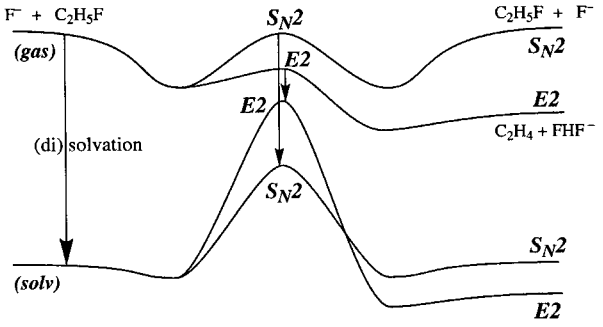

FIGURE 3. Schematic reaction energy profiles for unsolvated (gas) and (di)solvated (solv) S_N2 and *anti*-E2 reactions (after the TS, solvent molecules are transferred to the leaving group).

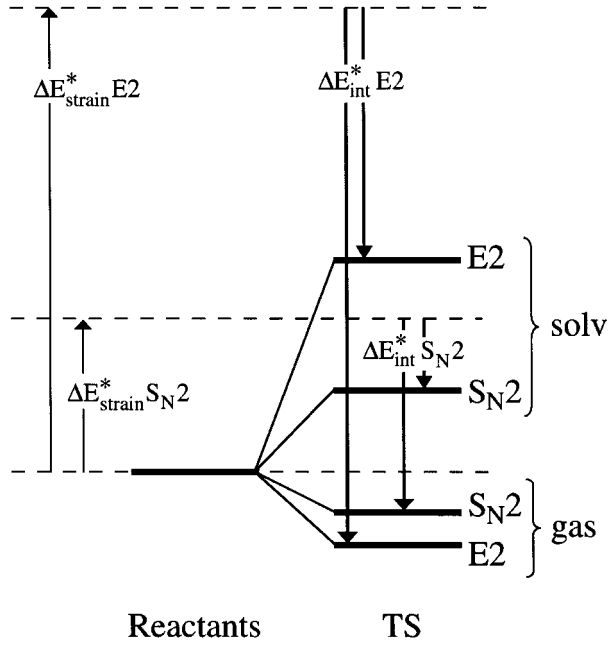

FIGURE 4. Base/substrate interaction (ΔE^*_{int}) and activation strain or deformation energy of the substrate (ΔE^*_{strain}) in E2 and S_N2 transition states for an unsolvated
(gas) and a solvated (solv) base.

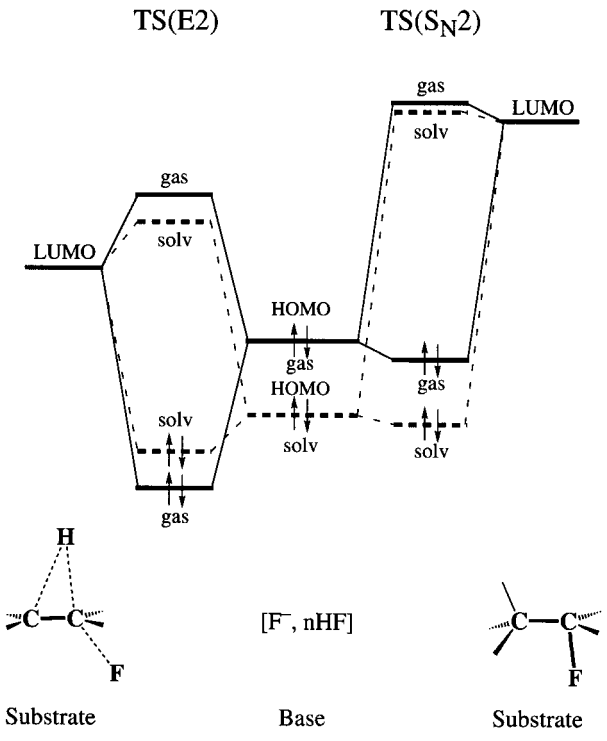

FIGURE 5. HOMO–LUMO interactions between the base (F^-) and the deformed substrate (C_2H_5F) in the S_N2 and *anti*-E2 transition states (solid lines: unsolvated base; dashed lines: solvated base). The lower energy LUMO of the strongly deformed substrate in the *anti*-E2 transition state leads to a more stabilizing interaction with the HOMO of the base. But, as the latter is stabilized on solvation, this interaction also undergoes the greatest weakening in absolute terms.

for this TS (Fig. 4). Now, the high activation strain (a characteristic of the elimination process, *vide supra*) shows up unfavorably, making the barrier of the solvated E2 elimination higher than that of the solvated S_N2 substitution (Fig. 4). We stress the equivalence of this view on solvation effects and the one based on differential solvation (*vide supra*). The advantage of analyzing the interaction between base (or nucleophile) and the deformed substrate (instead of that between solvent and reaction system) is that the same arguments used for understanding the effect of solvation may also shed some light on the effect of varying the base itself. For example, given that other factors do not change and leaving out overlap arguments (!), it is now easily seen that a stronger base (with a HOMO at high energy) will tend toward E2 elimination, whereas a weaker base (with a HOMO at low energy) will have an inclination toward S_N2 substitution.

Finally, we consider the effect of varying the substrate. As mentioned earlier, the LUMO of the present model substrate C_2H_5F is predestined to be attacked protophilically at H^{β} as it arises as the π-bonding combination of the empty $C^{\beta}H_3\cdot$ and the $\cdot C^{\alpha}H_2F$ e_x^* orbitals with a higher weight on the β-methyl group (Scheme 5). But, what happens if we substitute the leaving group with another one e.g., one that is more electronegative and/or more loosely bound to C^{α}? The effect of such a change will be a decrease in energy of the C—L antibonding e_x^* fragment orbital of $\cdot CH_2L$ (Scheme 7). If the effect is strong enough this will, in turn, result in a C_2H_5L LUMO with a higher amplitude on the C^{α} side of the substrate; that is, a typical backside lobe that is ideal for a nucleophilic S_N2 attack, as shown in Scheme 7.

These MO considerations are nicely confirmed by gas-phase experiments: Whereas, in general, E2 reactions dominate in gas-phase anion/molecule reactions, the S_N2 reaction prevails in the cation/molecule reaction between ammonia and the diethylmethyloxonium cation, which has a cationic leaving group [B = NH_3 and L = $OMeEt^+$ in eq. (4)].[26] In fact, what we have achieved is a simple connection between the E2 and the S_N2 mechanism. As the character of the LUMO of a substrate C_2R_5L changes from E2-like (Scheme 5) to S_N2-like (Scheme 7) the reactivity will shift from E2 to S_N2. Interestingly, the simple MO arguments also make the occurrence of E2C transition states plausible for the intermediate situation as the ''backside lobe'' begins to develop at C^{α} (Scheme 8). Analo-

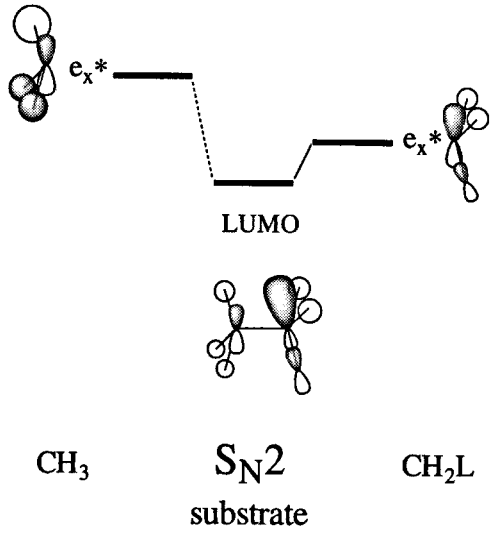

SCHEME 7. A substrate LUMO predestined for nucleophilic attack at C^{α}.

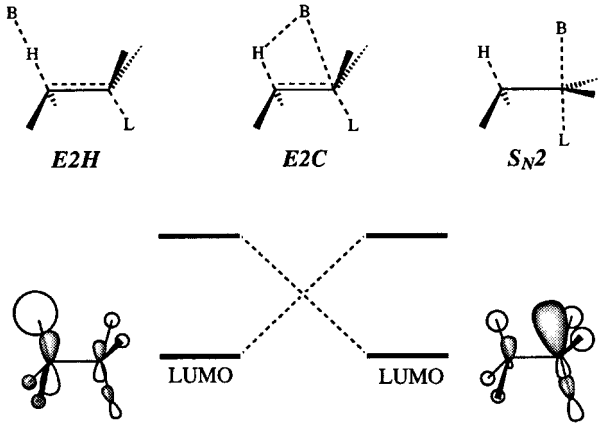

SCHEME 8. The E2–S_N2 mechanistic spectrum.

gously, one may wonder if, in turn, the S_N2 pathway will proceed via a TS with a certain degree of covalent nucleophile/H^{β} interaction (S_N2H mechanism?). In this way, using simple MO arguments, we arrive at an E2–S_N2 mechanistic spectrum, displayed in Scheme 8, which comprises not only the Bunnett–Cram E2H and the Winstein–Parker E2H–E2C, but also the S_N2–S_N1 mechanistic spectra.

Oxidative Addition Viewed as Frontside S_N2 Substitution

In the previous sections we dealt with elementary organic reactions (E2 and S_N2). Now, we extend our considerations to oxidative addition and reductive elimination (the reverse process), a class of fundamental reactions in *organometallic* chemistry [eq. (5)].[9d] These processes occur in nearly all homogeneous catalytic processes,[27] and are thus of major significance for synthetic chemistry and industrial processes. Consequently, they have been the subject of many experimental[27–31] and theoretical[32–35] studies:

$$ML_n + R{-}X \underset{\text{Red. E}}{\overset{\text{Oxid. Ad}}{\rightleftharpoons}} R{-}ML_n{-}X \qquad (5)$$

There are basically two different approaches to the investigation of oxidative addition. In the first approach, particular transition metal complexes are studied experimentally[27–29e–g] as well as theoretically,[32,33] using more or less realistic model systems in the latter case. In the second and more recent approach, the intrinsic reactivity of the metal ions or atoms is studied in the absence of ligands or solvent molecules, the effects of which may be added stepwise at later stages. Experimentally, this has been achieved using mass spectrometric[29,30] (metal ions) or spectroscopic[31] (metal atoms) techniques. Theoretical methods[9d,34,35] play a key role in this approach. They enable the study of model reaction systems, which are indispensable for achieving a real understanding of the reaction mechanism, but which often cannot be conducted experimentally.

In this section, we consider the intrinsic reactivity of palladium-d^{10} toward chloromethane, which has been studied at the BP86//Xα-VWN level of DFT using TZ2P (for Pd, Cl) and DZP (for C, H) basis sets.[9d] One may wonder if this model system reacts preferentially via direct oxidative insertion into the C—Cl bond [eq. (6a)] or via an S_N2-type mechanism which, after rearrangement of the expelled leaving group, yields the same oxidative addition product CH_3—Pd—Cl [eq. (6b)]:

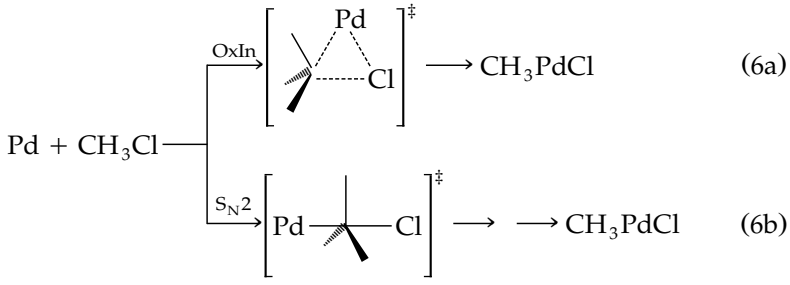

It is interesting to note in this context that our model reactions are closely related to the famous Monsanto acetic acid process and that the rate-determining step in this process is oxidative addition of a Rh(I) complex to CH_3I via nucleophilic substitution.[36] For a discussion of alternative mechanisms that are initiated by a single electron transfer (SET) from Pd to CH_3Cl, see ref. 9d.

The schematic reaction energy profiles for the oxidative insertion (OxIn) and nucleophilic substitution pathways of Pd + CH_3Cl are shown in Scheme 9.

A preference for the oxidative insertion pathway becomes apparent already on formation of the reactant complexes (Scheme 9). The reactant complex for oxidative addition, [CH_3Cl, Pd], is relatively stable, palladium being bound by −9.9 kcal/mol to chlorine (through a donor–acceptor interaction between the metal $4d_{z^2}$ and substrate σ^*_{C-Cl} orbitals), whereas the reactant complex for nucleophilic substitution, [Pd, CH_3Cl], is hold together by a rather weak agostic interaction of only −3.7 kcal/mol (between the palladium $4d_{xz}$ and a substrate σ^*_{C-H} orbital); see Table III and Figure 6. This trend continues, or is even reinforced, when we proceed to the respective transition states. The ''straight'' S_N2 substitution that leads to $PdCH_3^+ + Cl^-$ is not a viable reaction channel (not shown in Scheme 9). This process is highly endothermic (145.2 kcal/mol, not given in Table III), due to the charge separation, and proceeds without reverse activation barrier. The lowest energy pathway for nucleophilic substitution is one in which the anionic leaving group Cl^- keeps attached to and moves around the cationic $PdCH_3^+$ fragment toward the palladium atom, effectively yielding the oxidative addition product CH_3PdCl (Scheme 9). The associated activation energy is still quite high, 29.6 kcal/mol (Table III). Interestingly, in this transition state, TS(S_N2), the nucleophilic substitution is already more or less completed (Pd—C bond formed, C—Cl bond broken) and the reaction mode actually has the character of the Cl rearrangement (Fig. 6). None of these processes can compete with direct oxidative insertion (OxIn). Oxidative insertion proceeds via a very low activation barrier, which amounts to only 1.7 kcal/mol (Table III). The reaction energy for the formation of CH_3PdCl, via either S_N2 or OxIn, is −7.7 kcal/mol.

Why is the energy of TS(OxIn) so much lower? One important reason is the relatively small degree of deformation of the CH_3Cl substrate if compared with the S_N2 situation (see Fig. 6). The strong deformations that occur along the present

TABLE III.
Reactant Complexation and Activation Energies for Oxidative Insertion (OxIn) and Nucleophilic Substitution (S_N2) of Pd + CH_3Cl.[a]

Reaction	OxIn	S_N2
Reactant complexation	−9.9	−3.7
Activation energy	1.7	29.6

[a] In kilocalories per mole; BP86/TZ2P(C,H: DZP)// Xα-VWN/ TZ2P(C,H: DZP).

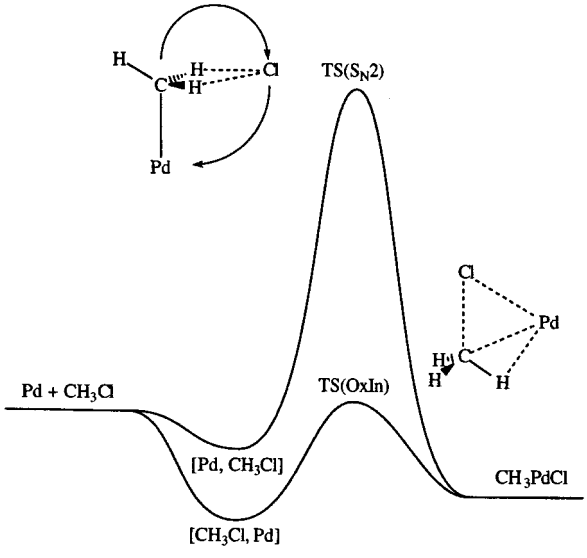

SCHEME 9. Reaction energy profiles for oxidative insertion and S_N2 substitution.

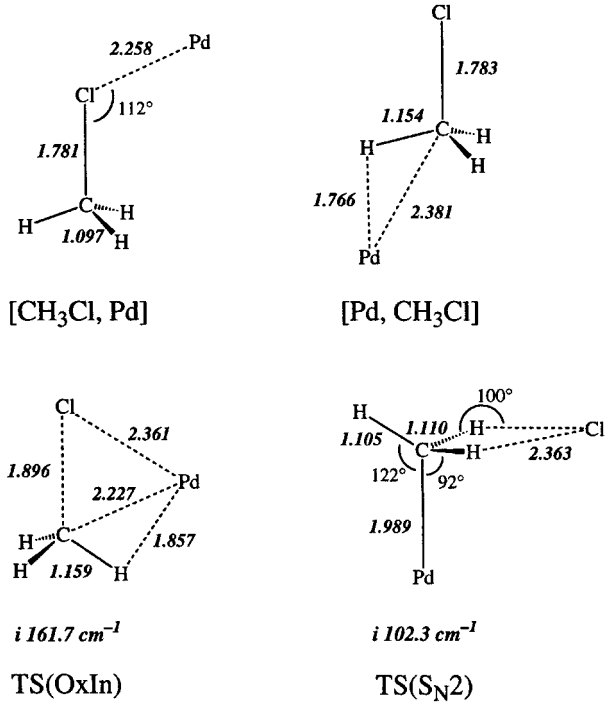

FIGURE 6. Geometries (in angstroms and degrees) for selected species on the oxidative-addition potential energy surface of Pd + CH_3Cl, together with imaginary frequencies for transition states (Xα-VWN/DZP level).

S_N2 pathways are related to the charge separation and the associated endothermicity, which leads to very late (''straight'' S_N2) or strongly rearranging transition states (S_N2 with Cl rearrangement, Scheme 9). Along the OxIn pathway, on the other hand, the positive Pd and negative Cl remain always close together and the TS is reached without much deformation. There is also a role for another factor that has to do with metal/substrate HOMO–LUMO overlap. To understand this, let us first consider the organic system $N + CH_3Cl$, where N represents a main group nucleophile, analogous to our organometallic $M + CH_3Cl$ system (where M = Pd). In general, the backside S_N2 substitution dominates in the organic reaction system,[13, 20b, c] which is explained on the basis of overlap arguments. Principally, a main group nucleophile, N, has a p- or sp^n-type HOMO, which favorably overlaps and interacts with the backside lobe of the σ^*_{C-Cl} orbital of the substrate. In the case of frontside attack, however, the interaction is very poor due to the well-known cancelation of overlap, as the HOMO lobe approaches on a nodal surface of σ^*_{C-Cl} (see Scheme 10).

But, as we have seen, such a frontside attack becomes favorable for a metal nucleophile, M (palladium). Here, in the context of overlap arguments, an important factor is that the d-type HOMO is ideally suited for frontside interaction with the σ^*_{C-Cl} of the substrate (Scheme 10). In this sense, oxidative insertion can be conceived as a frontside nucleophilic attack, which becomes feasible in the case of metal nucleophiles. We stress that this analogy should not be overrated. Of course, there are obvious differences between the reactions of $M + CH_3Cl$ and $N + CH_3Cl$, the most important one being the strong binding of the leaving group to the nucleophile in the final stage of the metal reaction. This difference is due to the special bonding capabilities of M, in particular the large flexibility to change the oxidation state. Nevertheless, one should also watch out not to exaggerate the differences. The reaction of $N + CH_3Cl$, too, can proceed via a product complex $[NCH_3^+, Cl^-]$, in which the expelled leaving group is bound either to N or CH_3. The interaction there is only weaker and more electrostatic in nature than in the metal case.

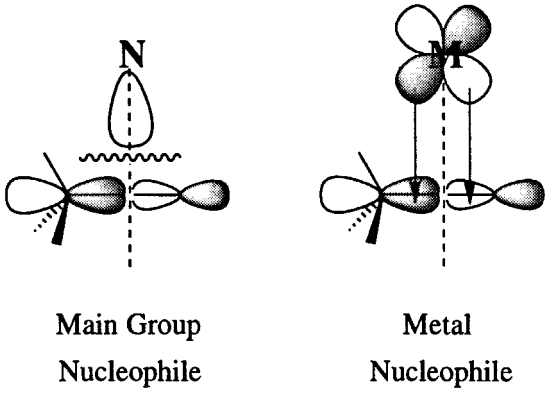

SCHEME 10. Frontside S_N2 attack for a main group and a metal nucleophile.

We have focused here on the *intrinsic* reactivity of palladium—that is, the reactivity of the uncoordinated metal center toward CH_3Cl. This is the necessary basis for the next step: the development of insight into the working of ligands. Ligands can affect the reactivity of a metal center in two different ways: (i) by changing the (relative) energy of the d-orbitals[9d]; and (ii) by changing their appearance or lobality.[32h, 37] Actually, there is yet another factor: ligands also determine (to a large extent) the sterical demand of a metal complex. The combined action of these mechanisms is responsible, for example, for the working of the square planar d^8 system $[Rh(CO)_2I_2]^-$; that is, the catalytic species of the well-known Monsanto acetic acid process. Contrary to our related but uncoordinated model system, $[Rh(CO)_2I_2]^-$ reacts in the rate-determining step of the Monsanto process specifically via backside S_N2 substitution with CH_3I, and this reactivity is further enhanced by prior coordination with I^-, under formation of the *penta*-coordinated d^8 complex $[Rh(CO)_2I_3]^{2-}$.[36b, d] Currently, we are undertaking efforts to analyze quantitatively the nature of ligand effects on the reactivity of different metal centers.[37] In this way, we hope to achieve a more rational design of catalysts.

Conclusions and Outlook

Kohn–Sham DFT constitutes an attractive, physically meaningful MO model that is perfectly suited for the discussion of issues concerning chemical bonding[4] and, as demonstrated in this work, chemical reactivity. We have shown how a detailed understanding of the electronic structure of a reaction system can help recognize certain characteristics of the process, yielding valuable mechanistic concepts. The conception of the base as a selective catalyst in E2 eliminations, for example, leads to a straightforward explanation for the stereochemistry of base-induced elimination reac-

tions (in general, trans coplanar). Furthermore, electronic structure considerations provide the so-called E2–S_N2 mechanistic spectrum (which constitutes a unified treatment of gas- and condensed-phase nucleophilic substitution and base-induced elimination reactions), and they make clear that oxidative addition may be conceived in some respect as an organometallic analog of the frontside S_N2 substitution in organic chemistry.

We have also introduced the idea of ''activation strain''; that is, the strain energy associated with deforming the reactants from their equilibrium structures to the geometry they acquire in the activated complex. This turns out to be a characteristic of a particular type of mechanism. It is high for E2 elimination (which proceeds through a more strongly deformed TS) and low for S_N2 substitution (which proceeds via a tighter, less deformed TS). The explicit recognition of this phenomenon as one factor that determines the activation barrier or competitiveness of a certain mechanism (*anti*-E2, *syn*-E2, S_N2) furnishes a helpful conceptual tool. The other factor is the interaction between the deformed reactants in the TS, which we designate here ''transition state interaction'' (i.e., $\Delta E^* = \Delta E^*_{\text{strain}} + \Delta E^*_{\text{int}}$). If the latter is strong, it can reverse the order in net activation energies, ΔE^*, of competing mechanisms relative to the order in activation strains, $\Delta E^*_{\text{strain}}$ (this is, e.g., the case for the gas-phase E2 and S_N2 reactions of $F^- + C_2H_5F$). But, as soon as ΔE^*_{int} becomes weak (e.g., on solvation of the base F^-) the activation strain, $\Delta E^*_{\text{strain}}$, begins to be the decisive principle that determines the height of the net barrier.

Finally, we note that the integration of accuracy, efficiency, *and* a transparent physical model into one single quantum-chemical method is not at all a matter of course. Quantum chemists have at times expressed their regret about the fact that the more sophisticated and accurate theoretical approaches become, the more elusive the understanding of these results appeared to be. Qualitative MO theory, on the other hand, has been, and still is, enormously successful in explaining and unifying the most diverse chemical phenomena, as documented by a number of excellent articles and textbooks.[5,6] However, somewhat unjustified, it suffers from a stigma of inaccuracy and semiempiricism. In this context, Kohn–Sham MO theory should not be viewed as a contender of qualitative MO theory, but as an extension, a logical next step in refinement and interpretative power that may reconcile the striving for accuracy and the quest for understanding.

Acknowledgment

I thank the Deutsche Forschungsgemeinschaft (DFG) for a Habilitationsstipendium.

References

1. (a) Dreizler, R. M.; Gross, E. K. U. Density Functional Theory, An approach to the Quantum Many-Body Problem; Springer: Berlin, 1990; (b) Parr, R. G.; Yang, W. Density-Functional Theory of Atoms and Molecules; Oxford University Press: New York, 1989; (c) Dunitz, J. D.; Hafner, K.; Houk, K. N.; Ito, S.; Lehn, J.-M.; Raymond, K. N.; Rees, C. W.; Thiem, J.; Vögtle, F. Topics in Current Chemistry, Vols. 180, 181; Springer: Berlin, 1996; (d) Hohenberg, P.; Kohn, W. Phys Rev 1964, 136, 864; (e) Kohn, W.; Sham, L. J. Phys Rev A 1965, 140, 1133.
2. (a) Ziegler, T. Can J Chem 1995, 73, 743; (b) Ziegler, T. Chem Rev 1991, 91, 651; (c) Labanowski, J. K.; Andzelm, J. W. (Eds.), Density Functional Methods in Chemistry; Springer: New York, 1991; (d) Laird, B. B.; Ross, R. B.; Ziegler, T. (Eds.) Chemical Applications of Density Functional Theory; American Chemical Society: Washington, DC, 1996; (e) Dunitz, J. D.; Hafner, K.; Houk, K. N.; Ito, S.; Lehn, J.-M.; Raymond, K. N.; Rees, C. W.; Thiem, J.; Vögtle, F. Topics in Current Chemistry, Vols. 182 and 183; Springer: Berlin, 1996; (f) Fonseca Guerra, C.; Snijders, J. G.; te Velde, G.; Baerends, E. J. Theor Chem Acc (in press); (g) te Velde, G. Thesis, Vrije Universiteit, Amsterdam, The Netherlands, 1990; (h) van den Hoek, P. J.; Kleyn, A. W.; Baerends, E. J. Comm Atom Mol Phys 1989, 23, 93.
3. (a) Curtiss, L. A.; Redfern, P. C.; Raghavachari, K.; Pople, J. A. J Chem Phys 1998, 109, 42; (b) Redfern, P. C.; Blaudeau, J.-P.; Curtiss, L. A. J Phys Chem A 1997, 101, 8701; (c) Becke, A. D. J Chem Phys 1993, 98, 1372, 5648; (d) J Chem Phys 1993, 97, 9173; (e) J Chem Phys 1992, 96, 2155; (f) Murray, C.; Laming, N. C.; Handy, N. C.; Chem Phys Lett 1992, 199, 551; (g) Perdew, J. P.; Chevary, J. A.; Vosko, S. H.; Jackson, K. A.; Pederson, M. R.; Singh, D. J.; Fiolhais, C. Phys Rev B 1992, 46, 6671.
4. Bickelhaupt, F. M.; Baerends, E. J. Rev Comput Chem (submitted).
5. (a) Hoffmann, R. Angew Chem 1982, 94, 725; Angew Chem Int Ed Engl 1982, 21, 711; (b) Hoffmann, R. Solids and Surfaces: A Chemists View of Bonding in Extended Structures; VCH: Weinheim, 1988.
6. (a) Rauk, A. Orbital Interaction Theory of Organic Chemistry; Wiley: New York, 1994; (b) Albright, T. A.; Burdett, J. K.; Whangbo, M.-H. Orbital Interactions in Chemistry; Wiley: New York, 1985; (c) Gimarc, B. M. Molecular Structure and Bonding; Academic: New York, 1979; (d) Fleming, I. Frontier Orbitals and Organic Chemical Reactions; Wiley: London, 1976.
7. (a) Shaik, S. S. J Am Chem Soc 1981, 103, 3692; (b) Pross, A.; Shaik, S. S. Acc Chem Res 1983, 16, 363; (c) Shaik, S. S.; Schlegel, H. B.; Wolfe, S. Theoretical Aspects of Physical Organic Chemistry; Wiley: New York, 1992; Chapter 3; (d) Shaik, S.; Hiberty, P. C. Adv Quantum Chem 1995, 26, 99.

See also: (e) McWeeny, R. Methods of Molecular Quantum Mechanics; Academic: London, 1992; Chapter 7.

8. (a) Bickelhaupt, F. M.; Nibbering, N. M. M.; van Wezenbeek, E. M.; Baerends, E. J. J Phys Chem 1992, 96, 4864; (b) Bickelhaupt, F. M.; Bickelhaupt, F. Chem Eur J (in press); (c) Bickelhaupt, F. M.; Diefenbach, A.; de Visser, S. V.; de Koning, L. J.; Nibbering, N. M. M. J Phys Chem A (in press); (d) Bickelhaupt, F. M.; Ziegler, T.; Schleyer, P. v. R. Organometallics 1996, 15, 1477; (e) Bickelhaupt, F. M.; van Eikema Hommes, N. J. R.; Fonseca Guerra, C.; Baerends, E. J. Organometallics 1996, 15, 2923.
9. (a) Bickelhaupt, F. M.; Nibbering, N. M. M.; Baerends, E. J.; Ziegler, T. J Am Chem Soc 1993, 115, 9160; (b) Bickelhaupt, F. M.; Baerends, E. J.; Nibbering, N. M. M. Chem Eur J 1996, 2, 196; (c) Bickelhaupt, F. M.; Diefenbach, A.; Baerends, E. J.; (to be submitted); (d) Bickelhaupt, F. M.; Ziegler, T.; Schleyer, P. v. R. Organometallics 1995, 14, 2288.
10. (a) Baerends, E. J.; Gritsenko, O. V. J Phys Chem A 1997, 101, 5383; (b) Baerends, E. J.; Gritsenko, O. V.; van Leeuwen, R. In Tsipis, C. A.; Popov, V. S.; Herschbach, D. R.; Avery, J. A. (Eds.) New Methods in Quantum Theory, Vol. 8; Kluwer: Dordrecht, 1996; (c) Baerends, E. J.; Gritsenko, O. V.; van Leeuwen, R. See ref. 2d, p. 20.
11. (a) Ziegler, T.; Rauk, A. Inorg Chem 1979, 18, 1558; (b) Ziegler, T.; Rauk, A. Inorg Chem 1979, 18, 1755; (c) Ziegler, T.; Rauk, A. Theor Chim Acta 1977, 46, 1.
12. (a) Morokuma, K. J Chem Phys 1971, 55, 1236; (b) Kitaura, K.; Morokuma, K. Int J Quantum Chem 1976, 10, 325; (c) Stone, A. J.; Erskine, R. W. J Am Chem Soc 1980, 102, 7185; (d) Bernardi, F.; Bottoni, A.; Mangini, A.; Tonachini, G. J Molec Struct (Theochem) 1981, 86, 163; (e) Post, D.; Baerends, E. J. J Chem Phys 1983, 78, 5663; (f) Dapprich, S.; Frenking, G. J Phys Chem 1995, 99, 9352.
13. (a) Lowry, T. H.; Richardson, K. S. Mechanism and Theory in Organic Chemistry, 2nd Ed.; Harper and Row: New York, 1981; (b) Carey, F. A.; Sundberg, R. J. Advanced Organic Chemistry, Part A; Plenum: New York, 1984; (c) March, J. Advanced Organic Chemistry, 4th Ed., Wiley: New York, 1992; (d) Isaacs, N. S. Physical Organic Chemistry, 2nd Ed., Longman: Harlow, UK, 1995. (e) Reichardt, C. Solvents and Solvent Effects in Organic Chemistry, 2nd Ed., VCH: Weinheim, 1988.
14. (a) Bartsch, R. A.; Závada, J. Chem Rev 1980, 80, 453; (b) Baciocchi, E. Acc Chem Res 1979, 12, 430; (c) Saunders, W. H., Jr. Acc Chem Res 1976, 9, 19; (d) Bunnett, J. F. Angew Chem 1962, 74, 731; (e) Cram, D. J.; Greene, F. D.; DePuy, C. H. J Am Chem Soc 1956, 78, 790; (f) McLennan, D. J. Tetrahedron 1975, 31, 2999; (g) Biale, G.; Cook, D.; Lloyd, D. J.; Parker, A. J.; Stevens, I. D. R.; Takahashi, J.; Winstein, S. J Am Chem Soc 1971, 93, 4735; (h) Parker, A. J.; Ruane, M.; Biale, G.; Winstein, S. Tetrahed Lett 1968, 2113; (i) Pirincciogluu, N.; Thibblin, A. J Am Chem Soc 1998, 120, 6512; (j) Meng, Q.; Thibblin, A. J Am Chem Soc 1995, 117, 9399.
15. (a) Bickelhaupt, F. M.; Buisman, G. H. J.; de Koning, L. J.; Nibbering, N. M. M.; Baerends, E. J. J Am Chem Soc 1995, 117, 9889; (b) Bickelhaupt, F. M. Recl Trav Chim Pays-Bas 1993, 112, 469; (c) Bickelhaupt, F. M.; de Koning, L. J.; Nibbering, N. M. M. J Org Chem 1993, 58, 2436; (d) Occhiucci, G.; Speranza, M.; de Koning, L. J.; Nibbering, N. M. M. J Am Chem Soc 1989, 111, 7387; (e) de Koning, L. J. Nibbering, N. M. M. J Am Chem Soc 1987, 109, 1715.
16. (a) DeTuri, V. F.; Hintz, P. A.; Ervin, K. M. J Phys Chem A 1997, 101, 5969; (b) Li, C.; Ross, P.; Szulejko, J. E.; McMahon, T. B. J Am Chem Soc 1996, 118, 9360; (c) Rabasco, J. J.; Gronert, S.; Kass, S. R. J Am Chem Soc 1994, 116, 3133; (d) Lum, R. C.; Grabowski, J. J. J Am Chem Soc 1992, 114, 9663; (e) Grabowski, J. J.; Lum, R. C. J Am Chem Soc 1990, 112, 607; (f) DePuy, C. H.; Gronert, S.; Mullin, A.; Bierbaum, V. M. J Am Chem Soc 1990, 112, 8650; (g) Jones, M. E.; Ellison, G. B. J Am Chem Soc 1989, 111, 1645; (h) Bierbaum, V. M.; Filley, J.; DePuy, C. H.; Jarrold, M. F.; Bowers, M. T. J Am Chem Soc 1985, 107, 2818; (i) Ridge, D. P.; Beauchamp, J. L. J Am Chem Soc 1974, 96, 637.
17. (a) Nibbering, N. M. M. Acc Chem Res 1990, 23, 279; (b) Riveros, J. M.; José, S. M.; Takashima, K. Adv Phys Org Chem 1985, 21, 197; (c) Olmstead, W. N.; Brauman, J. I. J Am Chem Soc 1977, 99, 4219; (d) Graul, S. T.; Bowers, M. T. J Am Chem Soc 1991, 113, 9696; (e) Cyr, D. M.; Posey, L. A.; Bishea, G. A.; Han, C.-C.; Johnson, M. A. J Am Chem Soc 1991, 113, 9697; (f) Wilbur, J. L.; Brauman, J. I. J Am Chem Soc 1991, 113, 9699.
18. (a) A negative activation energy does not imply the complete absence of any barrier. The reaction is still ''hampered'' by a statistical or entropic bottleneck that is associated with the decrease in the number of available quantum states (e.g., of translation, rotation, and vibration) as one goes from the separate, unbound reactants to the ''tightly'' bound transition states. See, for example, refs. 17a, b and McClelland, B. J. Statistical Thermodynamics; Chapman and Hall: London, 1973; Chapter 12. (b) As pointed out in ref. 9a, both the energetic and the entropic barrier reveal the same trend for the competition of the reaction pathways investigated for our gas-phase $F^- + C_2H_5F$ model system: (i) anti-E2 prevails over syn-E2 elimination; and (ii) E2 elimination dominates over S_N2 substitution.
19. (a) Nielsen, P. A.; Glad, S. S.; Jensen, F. J Am Chem Soc 1996, 118, 10577; (b) Hu, W.-P.; Truhlar, D. G. J Am Chem Soc 1996, 118, 860; (c) Glad, S. S.; Jensen, F. J Am Chem Soc 1994, 116, 9302; (d) Gronert, S.; Kass, S. R. J Org Chem 1997, 62, 7991; (e) Merrill, G. N.; Gronert, S.; Kass, S. R. J Phys Chem A 1997, 101, 208; (f) Gronert, S. J Am Chem Soc 1993, 115, 652; (g) J Am Chem Soc 1992, 114, 2349; (h) J Am Chem Soc 1991, 113, 6041; (i) Dewar, M. J. S.; Yuan, Y.-C. J Am Chem Soc 1990, 112, 2088, 2095; (j) Minato, T.; Yamabe, S. J Am Chem Soc 1988, 110, 4586; (k) J Am Chem Soc 1985, 107, 4621; (l) Pross, A.; Shaik, S. S. J Am Chem Soc 1982, 104, 187.
20. (a) Clary, D. C.; Palma, J. J Chem Phys 1997, 106, 575; (b) Glukhovtsev, M. N.; Pross, A.; Schlegel, H. B.; Bach, R. D.; Radom, L. J Am Chem Soc 1996, 118, 11258; (c) Deng, L.; Branchadell, V.; Ziegler, T. J Am Chem Soc 1994, 116, 10645; (d) Poirier, R. A.; Wang, Y.; Westatway, K. C. J Am Chem Soc 1994, 116, 2526; (e) Sini, G.; Shaik, S.; Hiberty, P. C. J Chem Soc Perkin Trans 2 1992, 1019; (f) Shi, Z.; Boyd, R. J. J Am Chem Soc 1991, 113, 1072; (g) Vande Linde, S. R.; Hase, W. L. J Phys Chem 1990, 94, 6148; (h) Carrion, F.; Dewar, M. J. S. J Am Chem Soc 1984, 106, 3531; (i) Wolfe, S.; Mitchell, D. J.; Schlegel, H. B. J Am Chem Soc 1981, 103, 7692, 7694.
21. (a) Ferguson, H. A.; Ferguson, J. D.; Holmes, B. E. J Phys Chem 1998, 102, 5393; (b) Kato, S.; Morokuma, K. J Chem Phys 1980, 73, 3900.

22. In addition, the leaving group is further removed from and therefore has less electrostatic repulsion with the attacking base in the anti-E2 transition state.
23. For experimental work on microsolvation, see: (a) Seeley, J. V.; Morris, R. A.; Viggiano, A. A.; Wang, H.; Hase, W. L. J Am Chem Soc 1997, 119, 577; (b) O'Hair, R. A. J.; Davico, G. E.; Hacaloglu, J.; Dang, T. T.; DePuy, C. H.; Bierbaum, V. M. J Am Chem Soc 1994, 116, 3609; (c) Freriks, I. L.; de Koning, L. J.; Nibbering, N. M. M.; J Org Chem 1992, 57, 5976; (d) van der Wel, H.; Nibbering, N. M. M.; Sheldon, J. C.; Hayes, R. N.; Bowie, J. H. J Am Chem Soc 1987, 109, 5823; (e) Hierl, P. M.; Ahrens, A. F.; Henchman, M.; Viggiano, A. A.; Paulson, J. F.; Clary, D. C. J Am Chem Soc 1986, 108, 3142; (f) Henchman, M.; Hierl, P. M.; Paulson, J. F. J Am Chem Soc 1985, 107, 2812; (g) Bohme, D. K.; Raksit, A. B. Can J Chem 1985, 63, 3007; (h) Bohme, D. K.; Raksit, A. B. J Am Chem Soc 1984, 106, 3447; (i) Henchman, M.; Paulson, J. F.; Hierl, P. M. J Am Chem Soc 1983, 105, 5509; (j) Bohme, D. K.; Mackay, G. I. J Am Chem Soc 1981, 103, 978.
24. For other theoretical work on microsolvation, see: (a) Hirao, K.; Kebarle, P. Can J Chem 1989, 67, 1261; (b) Ohta, K.; Morokuma, K. J Phys Chem 1985, 89, 5845; (c) Dewar, M. J. S.; Storch, D. M. J Chem Soc Chem Commun 1985, 94; (d) Jaume, J.; Lluch, J. M.; Oliva, A.; Bertrán, J. Chem Phys Lett 1984, 106, 232; (e) Yamabe, S.; Yamabe, E.; Minato, T. J Chem Soc Perkin Trans 2 1983, 1881. (f) Morokuma, K. J Am Chem Soc 1982, 104, 3732; (g) Novoa, J. J.; Mota, F.; Perez del Valle, C.; Planas, M. J Phys Chem 1997, 101, 7842.
25. (a) Hu, W.-P.; Truhlar, D. G. J Am Chem Soc 1994, 116, 7797; (b) Zhao, X. G.; Tucker, S. C.; Truhlar, D. G. J Am Chem Soc 1991, 113, 826; (c) Tucker, S. C.; Truhlar, D. G. J Am Chem Soc 1990, 112, 3338, 3347.
26. Occhiucci, G.; Speranza, M.; de Koning, L. J.; Nibbering, N. M. M. J Am Chem Soc 1989, 111, 7387.
27. (a) Elschenbroich, C.; Salzer, A. Organometallics. A Concise Introduction, 2nd Ed.; VCH: Weinheim, 1992; (b) Collman, J. P.; Hegedus, L. S.; Norton, J. R.; Finke, R. G. Principles and Applications of Organotransition Metal Chemistry; University Science Books: Mill Valley, CA, 1987.
28. (a) Rendina, L. M.; Puddephatt, R. J. Chem Rev 1997, 97, 1735; (b) Gandelman, M.; Vigalok, A.; Shimon, L. J. W.; Milstein, D. Organometallics 1997, 16, 3981; (c) Wick, D. D.; Goldberg, K. I. J Am Chem Soc 1997, 119, 10235; (d) Crabtree, R. H. Chem Rev 1995, 95, 987; (e) Grushin, V. V.; Alper, H. Chem Rev 1994, 94, 1047; (f) Wright, M. W.; Smalley, T. L.; Welker, M. E.; Rheingold, A. L. J Am Chem Soc 1994, 116, 6777; (g) Sakakura, T.; Sodeyama, T.; Sasaki, K.; Wada, K.; Tanaka, M. J Am Chem Soc 1990, 112, 7221; (h) Casalnuovo, A. L.; Calabrese, J. C.; Milstein, D. J Am Chem Soc 1988, 110, 6738; (i) Janowicz, A. H.; Bergman, R. G. J Am Chem Soc 1983, 105, 3929.
29. (a) Schwarz, J.; Heinemann, C.; Schröder, D.; Schwarz, H. Helv Chim Acta 1996, 79, 1; (b) Carpenter, C. J.; van Koppen, P. A. M.; Bowers, M. T. J Am Chem Soc 1995, 117, 10976; (c) Chen, Y.-M.; Clemmer, D. E.; Armentrout, P. B. J Am Chem Soc 1994, 116, 7815; (d) Wesendrup, R.; Schröder, D.; Schwarz, H. Angew Chem 1994, 105, 1232; (e) van den Berg, K. J.; Ingemann, S.; Nibbering, N. M. M.; Gregor, I. K.; Rapid Common Mass Spectrom 1993, 7, 769; (f) Eller, K.; Schwarz, H. Chem Rev 1991, 91, 1121; (g) Armentrout, P. B.; Beauchamp, J. L. Acc Chem Res 1989, 22, 315.
30. (a) Chowdhury, A. K.; Wilkins, C. L. J Am Chem Soc 1987, 109, 5336; (b) Weil, D. A.; Wilkins, C. L. J Am Chem Soc 1985, 107, 7316; (c) Jones, R. W.; Staley, R. H. J Phys Chem 1982, 86, 1669; (d) Jones, R. W.; Staley, R. H. J Am Chem Soc 1980, 102, 3794.
31. (a) Chertihin, G. V.; Andrews, L. J Am Chem Soc 1994, 116, 8322; (b) Ritter, D.; Weisshaar, J. C. J Am Chem Soc 1990, 112, 6425; (c) Mitchell, S. A.; Hackett, P. A. J Chem Phys 1990, 93, 7822.
32. (a) Bickelhaupt, F. M.; Radius, U.; Ehlers, A. W.; Hoffmann, R.; Baerends, E. J. New J Chem 1998, 1; (b) Radius, U.; Bickelhaupt, F. M.; Ehlers, A. W.; Goldberg, N.; Hoffmann, R. Inorg Chem 1998, 37, 1080; (c) Cotton, F. A.; Feng, X. J Am Chem Soc 1997, 119, 7514; (d) Yoshizawa, K.; Ohta, T.; Yamabe, T.; Hoffmann, R. J Am Chem Soc 1997, 119, 12311; (e) Ehlers, A. W.; Dapprich, S.; Vyboishchikov, S. F.; Frenking, G. Organometallics 1996, 15, 105; (f) Irikura, K. K.; Goddard, W. A., III. J Am Chem Soc 1994, 116, 8733; (g) Perry, J. K.; Goddard, W. A., III. J Am Chem Soc 1994, 116, 5013; (h) Bickelhaupt, F. M.; Baerends, E. J.; Ravenek, W. Inorg Chem 1990, 29, 350; (i) Koga, N.; Morokuma, K. Chem Rev 1991, 91, 823; (j) Ziegler, T.; Tschinke, V.; Fan, L.; Becke, A. D. J Am Chem Soc 1989, 111, 9177.
33. (a) Griffin, T. R.; Cook, D. B.; Haynes, A.; Pearson, J. M.; Monti, D.; Morris, G. E. J Am Chem Soc 1996, 118, 3029; (b) Aullón, G.; Alvarez, S. Inorg Chem 1996, 35, 3137; (c) Hinderling, C.; Feichtinger, D.; Plattner, D. A.; Chen, P. J Am Chem Soc 1997, 119, 10793; (d) Cui, Q.; Musaev, D. G.; Morokuma, K. J Chem Phys 1998, 108, 8418; (e) Su, M.-D.; Chu, S.-Y. Inorg Chem 1998, 37, 3400.
34. (a) Hendrickx, M.; Ceulemans, M.; Gong, K.; Vanquickenborne, L. J Phys Chem A 1997, 101, 8540; (b) Perry, J. K.; Ohanessian, G.; Goddard, W. A., III. Organometallics 1994, 13, 1870; (c) Siegbahn, P. E. M. Organometallics 1994, 13, 2833; (d) Siegbahn, P. E. M.; Blomberg, M. R. A.; Svensson, M. J Am Chem Soc 1993, 115, 1952.
35. (a) Siegbahn, P. E. M. J Am Chem Soc 1994, 116, 7722; (b) Siegbahn, P. E. M.; Blomberg, M. R. A.; Svensson, M. J Phys Chem 1993, 97, 2564; (c) Blomberg, M. R. A.; Siegbahn, P. E. M.; Svensson, M. Inorg Chem 1993, 32, 4218; (d) Siegbahn, P. E. M.; Blomberg, M. R. A.; Svensson, M. J Am Chem Soc 1993, 115, 4191; (e) Blomberg, M. R. A.; Siegbahn, P. E. M.; Svensson, M. J Am Chem Soc 1992, 114, 6095; (f) Svensson, M.; Blomberg, M. R. A.; Siegbahn, P. E. M. J Am Chem Soc 1991, 113, 7076.
36. (a) Ref. 27b, Chapter 12; (b) Hickey, C. E.; Maitlis, P. M. J Chem Soc Chem Commun 1984, 1609; (c) Forster, D. Adv Organometal Chem 1979, 17, 255; (d) Forster, D. J Am Chem Soc 1975, 97, 951; (e) J Am Chem Soc 1976, 98, 846.
37. Bickelhaupt, F. M. Unpublished results.